PAPER

Synthesis and structures of molecular beryllium Grignard analogues featuring terminal and bridging pseudohalides†

Corinna Czernetzki, [ID] a,b Merle Arrowsmith, [ID] a,b Malte Jürgensen,a,b Stephan Hagspiel [ID] a,b and Holger Braunschweig [ID] *a,b

The carbene-stabilised beryllium Grignards [(CAAC)BeBrR] (R = CAACH **1a**, Dur **1b**; CAAC/H = 1-(2,6-di-*iso*propylphenyl)-2,2,4,4-tetramethylpyrrolidin-2-yl/idene; Dur = 2,3,5,6-tetramethylphenyl) undergo salt metathesis with various pseudohalide salt precursors. Whereas with [NaNCS] the thiocyanato Grignards [(CAAC)Be(NCS)R] (R = CAACH **2a**, Dur **2b**) are obtained selectively, salt metatheses with [Na(OCP)(dioxane)$_{2.3}$] and [K(OCN)] are fraught with side reactions, in particular scrambling of both neutral and anionic ligands, leading to complex product mixtures, from which the first examples of beryllium phosphaethynolate Grignards [(thf)$_2$(CAACH)Be(OCP)] (**3**) and [(CAAC)Be(OCP)R] (R = CAACH **4a**, Dur **4b**), as well as the isocyanate-bridged hexamer [(CAAC)BrBe(1,3-μ-OCN)]$_6$ (**7**) were determined as the main products. The complexity of possible side reactions is seen in complex **5**, a byproduct of the salt metathesis of **1b** with [Na(OCP)(dioxane)$_{2.3}$], which hints at radical redox processes, OCP homocoupling, OCP coupling with CAAC, as well as OCP insertion into the Be–R bond. Finally, the unstable, tetrameric cyano-bridged beryllium Grignard [(thf)(CAACH)Be(1,2-μ-CN)] (**8**) was obtained by salt metathesis of **1a** with [Na/KSeCN] alongside one equiv. CAAC═Se. The new complexes were characterised by heteronuclear NMR and IR spectroscopy, as well X-ray crystallography.

Introduction

Named a century ago after their chemical resemblance with the halides,[1] pseudohalides have since found applications ranging from organic cross-coupling or carboxylation reagents to ionic liquids and solar cell materials.[2–7] Linear pseudohalogen anions, such as CN^-, N_3^- or NCO^-, are ambiphilic and thus capable of coordinating *via* both ends. As a result, the homoleptic alkaline earth pseudohalides, $[AeY_2]$, are usually oligomers featuring bridging pseudohalides.[8]

Whereas the chemistry of classical and heavier Grignard reagents, [RAeX] (R = organyl, X = halide), is one of the mainstays of organic and inorganic chemistry,[9–13] that of their pseu-

dohalide derivatives is virtually unknown. The difficulties in isolating well-defined molecular group 2 Grignard analogues of the form [L$_n$AeRY] (L = neutral donor), featuring a terminal unsymmetrical pseudohalide ligand (*e.g.* CN^-, NCO^-, NCS^-, OCP^-) are threefold: (1) the ambidentate nature of unsymmetrical pseudohalides, frequently resulting in the formation of mixtures of linkage isomers or oligomers,[14] (2) the tendency of heteroleptic group 2 complexes to undergo Schlenk-type ligand scrambling,[15] which results in the often irreversible formation of homoleptic compounds, and (3) the propensity of some unsymmetrical pseudohalides, like CN or NCO, to undergo unwanted nucleophilic addition reactions.[16]

In 1974, Klopsch and Dehnicke were the first to synthesise dianionic organomagnesium pseudohalides of the form [{Me$_2$Mg}$_2$(μ-Y)]$^{2-}$ and [{Me$_2$Mg(η^1-Y)}$_2$]$^{2-}$ (Y = CN, N$_3$, NCO), as determined by IR spectroscopy.[17] In 1998 Böhland reported the first neutral thiocyanate and selenocyanate Grignards [(thf)$_n$Mg(NCE)R] (**I^R-E**, R = Et, Ph, E = S, Se, Fig. 1A), which undergo Schlenk equilibration to the homoleptic species in solution.[18] Much more recently, Gilliard isolated the first phosphaethynolate Grignard, **II**, stabilised against ligand redistribution by two bulky N-heterocyclic carbenes (NHCs).[19] To date, complex **II** is the only structurally characterised pseudohalide Grignard analogue.

*a*Institute for Inorganic Chemistry, Julius-Maximilians-Universität Würzburg, Am Hubland, 97074 Würzburg, Germany.
E-mail: h.braunschweig@uni-wuerzburg.de
*b*Institute for Sustainable Chemistry & Catalysis with Boron, Julius-Maximilians-Universität Würzburg, Am Hubland, 97074 Würzburg, Germany
†Electronic supplementary information (ESI) available: Synthetic procedures, NMR spectra, and X-ray crystallographic details. CCDC 2379134–2379141. For ESI and crystallographic data in CIF or other electronic format see DOI: https://doi.org/10.1039/d4dt02457e
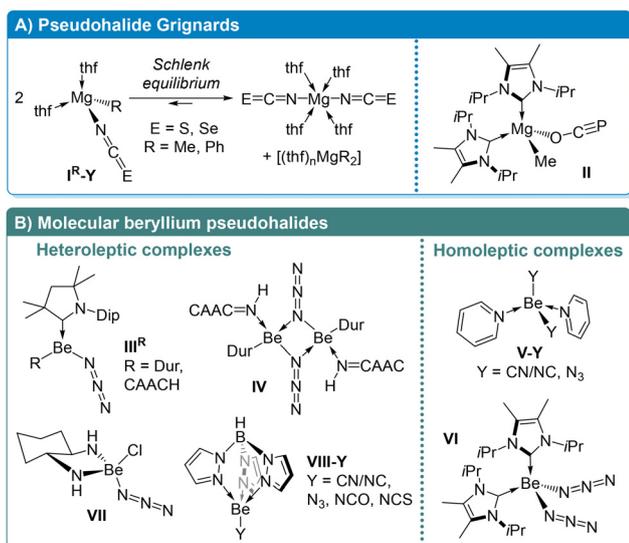
Fig. 1 Examples of pseudohalide Grignards and molecular beryllium pseudohalides. Dip = 2,6-di*iso*propylphenyl, Dur = 2,3,5,6-tetramethyl-phenyl (= duryl), CAAC = 1-(2,6-di*iso*propylphenyl)-2,2,4,4-tetramethyl-pyrrolidin-5-ylidene.

Long neglected due to the high toxicity of its compounds,‡ the last decade has seen a revival of organoberyllium chemistry,[20–22] not least because of the landmark syntheses of the first Be(0) and Be(I) complexes.[23–27] As the least polarisable and smallest of the group 2 dications, Be^{2+} forms largely covalent bonds with carbon. As a result, beryllium-based Grignard complexes tend to be more stable than their magnesium analogues towards Schlenk equilibration.[28,29] Our group recently reported the first beryllium-based pseudohalide Grignards, the cyclic alkyl (amino)carbene (CAAC)-stabilised terminal azide complexes **III^R** and the imine-stabilised azide-bridged dimer **IV** (Fig. 1B).[30] Beyond this, only a handful of molecular beryllium pseudohalides have been reported, including tetrahedral homoleptic terminal cyanide, azide and thiocyanate complexes of the form [L$_2$BeY$_2$] (L = pyridine (**V-Y**), amine, imine, NHC (**VI**)),[30–32] as well as a heteroleptic diamine-supported chloroberyllium azide (**VII**),[33] and the tris(pyrazolyl) borate (Tp) complexes [(Tp)BeY] (**VIII-Y**, Y = CN, N$_3$, NCS).[34,35]

In this study we report the synthesis, spectroscopic and structural characterisation of a range of monomeric and oligomeric Lewis-base-stabilised beryllium pseudohalide Grignards, including the first structurally characterised beryllium phosphaethynolates and isocyanates.

Results and discussion

Synthesis of beryllium pseudohalides

The dropwise addition of 1 equiv. [NaNCS] in THF to **1a**[26] and **1b**[36] in THF at −78 °C, followed by stirring for 3 h at room temperature yielded, after workup, the corresponding beryllium thiocyanates **2a** and **2b** as yellow (75%) and colourless (58%) solids, respectively (Scheme 1a). Their ^{9}Be NMR spectra show a broad resonance at 15.5 ($\omega_{1/2}$ (full width at half maximum) ≈ 420 Hz) and 14.8 ($\omega_{1/2}$ ≈ 210 Hz) ppm, respectively, *ca.* 5 ppm upfield-shifted from that of their respective precursors ($\delta_{^9Be}$ = 20.0 (**1a**), 18.7 (**1b**) ppm). Their ^{13}C NMR $C_{carbene}$ resonances at 249.6 and 240.1 ppm, respectively, are virtually identical to that of their respective precursors ($\delta_{^{13}C}$ = 249.7 (**1a**), 240.1 (**1b**) ppm). The ^{13}C NMR resonance of the N*C*S moiety could not be detected, presumably owing to excessive broadening caused by strong coupling with the nearby quadrupolar ^{9}Be and ^{14}N nuclei. Complexes **1a** and **1b** represent the first examples of tricoordinate beryllium thiocyanates, previous examples being limited to tetracoordinate neutral[35] or ionic complexes.[37] The solid-state IR spectra of **2a** and **2b** show a single, very intense and relatively broad N=C stretching band at 2100 and 2089 cm^{-1}, respectively, in the same range as other molecular and ionic terminal beryllium thiocyanates (ν(N=C) = 2065–2117 cm^{-1}).[35,37] Compounds **2a/b** were stable in benzene up to 80 °C.

The ^{9}Be and ^{31}P NMR spectra of the reaction mixture of **1a** with [Na(OCP)(dioxane)$_{2.3}$] showed the formation of two main products in a 96 : 4 ratio. Workup revealed the major one of these to be the colourless tetracoordinate complex [(thf)$_2$(CAACH)Be(OCP)], present as a mixture of two isomers, **3** and **3′**, in an 88 : 12 ratio, respectively ($\delta_{^9Be}$ = 7.1 (s, $\omega_{1/2}$ ≈ 150 Hz, **3′**), 4.7 (s, $\omega_{1/2}$ ≈ 145 Hz, **3**) ppm; $\delta_{^{31}P}$ = −342.6 (s) ppm, Scheme 1b).§ Recrystallisation from pentane also yielded a few crystals of the expected tricoordinate CAAC-stabilised species **4a** ($\delta_{^{31}P}$ = −339.4 ppm) as determined by X-ray crystallography (*vide infra*).¶ The ^{1}H NMR spectrum of the major rotamer, **3**, confirms the presence of two THF ligands, with 8H multiplets at 3.41 and 1.90 ppm, as well as the chiral CAACH ligand with its characteristic 1H singlet at 2.68 ppm for the Be*CH* resonance. The terminal nature and Be–O bonding of the OCP ligand is attested by a broad ^{13}C{^{1}H} NMR doublet at 156.6 ($^1J_{C–P}$ = 13.3 Hz, O*C*P) and a ^{31}P{^{1}H} singlet at −342.6 (OC*P*) ppm. These are upfield- and downfield-shifted, respectively, from the range of ^{13}C{^{1}H} and ^{31}P{^{1}H} NMR O*C*P resonances observed for molecular terminal magnesium phosphaethynolates ($\delta_{^{13}C}$ = 161–169 ppm, $\delta_{^{31}P}$ = −365–(−386) ppm).[19,38,39] This may be rationalised by the much higher charge density of the

---

‡ **Caution!** Beryllium and its compounds are regarded as toxic and carcinogenic. Because the biochemical mechanisms that cause beryllium-associated diseases are still unknown, special (safety) precautions are strongly advised.[65,66]

§ The same reaction carried out in benzene instead of THF to avoid CAAC-THF ligand scrambling proved much less selective. The low isolated yield of **3** of 33% is due to the difficulty in separating **3** from the CAAC ligand released during the reaction, as both have very similar solubility in pentane.

¶ The calculated ^{9}Be NMR shift of **4a** at the B3LYP-D3(BJ)-def2-SVP level of theory using **2b** ($\delta_{^9Be}$ = 14.8 ppm) as a reference is 14.6 ppm, therefore **4a** is unlikely to be the minor product observed at $\delta_{^9Be}$ = 7.1 ppm.
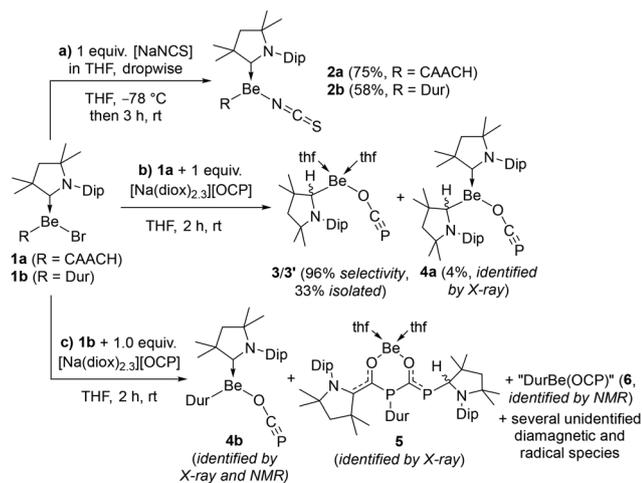
Scheme 1 Synthesis of beryllium isothiocyanates and phosphaethyno-lates. Isolated yields in parentheses.

Be^{2+} dication, which draws electron density away from the terminal phosphorus atom, thus favouring the O–C≡P over the O^+=C=P$^-$ resonance structure. Furthermore, magnesium phospaethynolates display significantly larger ^{13}C–^{31}P coupling constants ($^1J_{C-P}$ = 25–60 Hz),[19,38,39] the smallest one being observed for complex **II** (see Fig. 1A).[19] Similarly small OCP ^{13}C–^{31}P coupling constants to that of **3** have been observed in iPr$_3$Si(OCP),[40] a β-diketiminate-stabilised scandium OCP complex (both $^1J_{C-P}$ = 10 Hz),[41] and an OCP-substituted 1,3-dihydrodiazaborole ($^1J_{C-P}$ = 17 Hz).[42] Smaller ^{13}C–^{31}P coupling constants are associated with a higher degree of phosphaethynolate O–C≡P bonding, whereas larger ones are indicative of increased phosphaketene O=C=P bonding,[43] thereby confirming that the Be–O–C≡P resonance structure is highly dominant in **3**. This was also confirmed by IR spectroscopy of **3/3′**, which shows an intense and relatively broad asymmetric OCP stretching band at 1728 cm^{-1}, in the lower range of those observed for terminal magnesium phosphaethynolates (ν(OCP)$_{asym}$ = 1727–1770 cm^{-1})[19,38,39] and similar to that of [(18-crown-6)K(OCP)] (ν(OCP)$_{asym}$ = 1730 cm^{-1}).[44] Compound **3/3′** was stable in benzene up to 60 °C but decomposed unselectively upon UV irradiation.

The reaction of **1b** with [Na(OCP)(dioxane)$_{2.3}$] proved much less selective. The ^9Be NMR spectrum of the crude reaction mixture after 30 min at room temperature evidenced the formation of a least two tricoordinate (δ_{9Be} = 17.4 (br), 14.1 (br) ppm) and two tetracoordinate (δ_{9Be} = 4.7 (s), 1.8 (s) ppm) beryllium complexes.[45] The two main products observed by ^{31}P NMR spectroscopy feature a sharp singlet at −328.6 (*ca.* 46%) ppm, which fits a phosphaethynolate complex, and a very broad resonance at −343.1 ppm ($\omega_{1/2}$ ≈ 320 Hz, *ca.* 36%), suggesting Be–P bonding, respectively, alongside several other minor unidentified products. Furthermore, the unexpected intense colouration of the reaction mixture (first dark purple, then dark brown), usually the hallmark of radical CAAC complexes,[23,26,27,46] prompted us to measure a solution EPR

spectrum. The latter indeed showed the presence of at least three radical species, none of which could be identified further, but which highlight that this seemingly simple salt metathesis is accompanied by complex redox processes.

Recrystallisation of the crude product mixture by diffusion of hexane into a saturated benzene solution yielded a few crystals of the tricoordinate beryllium phosphaethynolate **4b**, which was identified as the major reaction product (δ_{9Be} = 14.1 (br, $\omega_{1/2}$ ≈ 470 Hz) ppm; δ_{31P} = −328.6 (s) ppm).|| **4b** systematically cocrystallised with 30% of another tetracoordinate beryllium complex (**6**, δ_{9Be} = 1.4 (br, $\omega_{1/2}$ ≈ 280 Hz) ppm; δ_{31P} = −339.6 (s) ppm), containing a 1 : 1 ratio of Dur and terminal OCP substituents, as determined by ^1H and ^{31}P NMR spectroscopy. Unfortunately, the constitution of this complex could not be elucidated further. Further crystallisation yielded a few crystals suitable for X-ray diffraction analysis of an unexpected side-product, complex **5** (see Fig. S30 in the ESI†), which evidences the insertion of an OCP fragment into the Be–Dur bond, coupling of two PCO ligands *via* P–C bond formation, as well as C_{CAAC}–C_{PCO} and C_{CAACH}–P_{PCO} bond formation, the CAACH residue suggesting the involvement of a CAAC radical and hydrogen atom abstraction.

The lack of selectivity of the reaction between **1b** and [Na(OCP)(dioxane)$_{2.3}$] reflects the multitude of possible side-reactions when attempting to synthesise main group phosphaethynolates, including ether cleavage of the dioxane ligands of [Na(OCP)(dioxane)$_{2.3}$],[19] OCP coupling,[42,47] CAAC–PCO coupling,[48,49] aryl transfer to the phosphorus atom from an s-block aryl reagent,[42,50] photoinduced CO extrusion with radical P–P coupling,[42,51,52] or photoinduced [PCO]• extrusion.[51] Similar light-induced redox processes might be at play here and responsible for the radical species observed by EPR spectroscopy.

Attempts to obtain an isocyanate derivative of **1a** by salt metathesis with [KOCN] at 60 °C yielded a mixture of four tetracoordinate beryllium complexes (δ_{9Be} = 8.8, 7.0, 4.0, 2.0 ppm) in various ratios depending on the reaction time. Multiple attempts to improve the selectivity of the reaction by changing equivalents, solvent, temperature and reaction time failed. Recrystallisation of the crude product mixture from benzene yielded a few colourless single crystals of the hexameric complex **7**, which is comprised of six [(CAAC)BeBr(OCN)] units, the OCN ligands bridging between two adjacent beryllium centres, thus forming a 24-membered (BeOCN)$_6$ ring (Scheme 2a). It is noteworthy that **7** has lost the CAACH substituent but still contains an unreacted bromide substituent, suggesting the involvement of temperature- and/or sterics-induced Schlenk-type equilibria, which have been observed in beryllium Grignard analogues, albeit to a lesser degree than their magnesium counterparts.[28,29] Attempts to obtain **7** more selectively by salt metathesis with (CAAC)BeBr$_2$, however, proved unsuccessful. Taking into account potential ligand

---

|| Compound **4b** slowly decomposed within the reaction mixture upon exposure to light.

Dalton Transactions

Paper
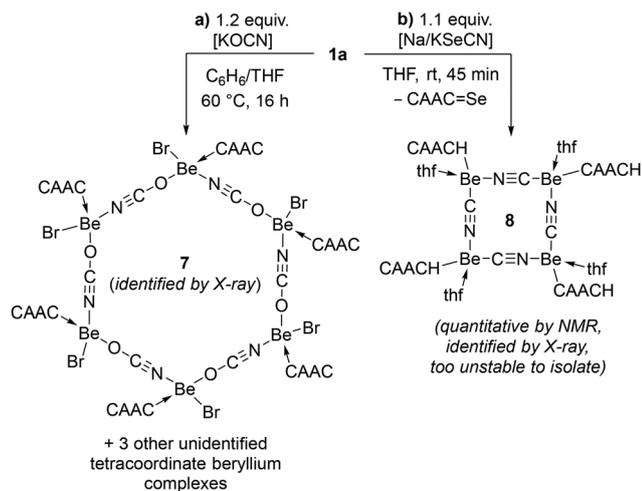
Scheme 2 Synthesis of beryllium isocyanate and cyanoberyllium oligomers.

exchange processes and steric effects, the other products observed by ^{9}Be NMR spectroscopy are likely to be either similarly OCN-bridged hexamers of the form [LBeY(1,3-μ-OCN)]$_6$ (L = CAAC, Y = η^1-OCN; L = THF, Y = CAACH), or dimeric [(THF)Be(OCN)]$_2$, by analogy to Buchner's [(Me$_2$S)Be(η^1-OCN) (μ-OCN)]$_2$ (δ$_{9Be}$ = 7.0 ppm),[35] or mononuclear terminal beryllium isocyanates of the form [(THF)$_2$BeY(η^1-OCN)] (Y = CAACH, η^1-OCN), akin to complex 3 and **VIII-OCN** (see Fig. 1B).[35]

Finally, the salt metathesis of **1a** with the heavier isocyanate analogues [NaSeCN] and [KSeCN] proceeded selectively at room temperature in THF under elimination of CAAC=Se,[53] to yield a single beryllium-containing product with a broad ^{9}Be

NMR resonance at 3.4 ppm ($\omega_{1/2} \approx 440$ Hz). Recrystallisation from pentane at −30 °C yielded light brown crystals of the tetramer **8**, which is comprised of four [(THF)Be(CAACH)(CN)] units, the CN ligands bridging between two adjacent beryllium centres, thus forming a 12-membered (BeCN)$_4$ ring (Scheme 2b). The ^{9}Be NMR shift of **8** is slightly downfield-shifted from those observed for the coordination isomers **VIII-CN** and **VIII-NC** at 1.9 and 1.6 ppm, respectively.[35] Complex **8** proved extremely sensitive, even decomposing on the diffractometer at −173 °C. A full *in-situ* NMR-spectroscopic characterisation of the reaction mixture was marred by the fact that all four CN linkers of the (BeCN)$_4$ ring are flip-disordered, yielding a complex mixture of isomers. Attempts to obtain a cyanoberyllium complex more directly by salt metathesis of **1a** with [NaCN] or [KCN] required higher reaction temperatures (60–80 °C) and led to intractable product mixtures.

X-ray crystallographic analyses

X-ray diffraction analyses provided the solid-state structures of **2a**, **2b**, **3**, **4a**, **4b**, **5**, **7** and **8**. Due to excessive twinning, poor diffraction and rapid crystal decomposition the data for **8** is of insufficient quality to be discussed but provide conclusive proof of connectivity (Fig. S32 in the ESI†). Selected structural data for **2a**, **2b**, **3**, **4a**, **4b** and **7** are provided in Table 1, together with relevant NMR- and IR-spectroscopic data.

Complexes **2a**, **2b**, **4a** and **4b** (Fig. 2) are trigonal-planar (Σ∠Be *ca.* 360°) and display a terminal pseudohalide ligand. The Be–C1 bond length to the neutral CAAC ligand (1.810(2)–1.823(2) Å) is similar to that in the precursors **1a** and **1b** (1.798 (2), 1.829(2) Å).[26,36] The CAAC and CAACH ligands in **2a** and **4a** adopt an *anti* conformation relative to each other so as to

Table 1 ^{9}Be NMR shifts (δ_{9Be}, ppm) with their full widths at half-maximum ($\omega_{1/2}$, Hz), pseudohalide IR stretching frequencies (ν_{ps}, cm^{-1}), as well as selected bond lengths (Å), bond angles (°) and absolute values of torsion angles (°) for the beryllium complexes presented herein

	1a^{a,b}	**1b**^{a,c}	**3**^{b,d,e}	**4a**^{b,d,f}	**4b**^{c,f}	**7**^{g,h}
δ_{9Be}	15.5	14.8	4.7	n.d.^{i}	17.0	n.d.
$\omega_{1/2}$	420	210	150	n.d.	340	n.d.
ν_{ps}	2100	2089	1727	n.d.	1691	n.d.
N1–C1	1.3011(15)	1.2967(16)	—	1.302(2)	1.2998(18)	1.292(4)–1.296(4)
N2–C3	1.4833(15)	—	1.5151(17)	1.486(2)	—	—
Be–C1	1.811(2)	1.823(2)	—	1.813(3)	1.810(2)	1.827(5)–1.836(5)
Be–C3	1.7655(19)	1.743(2)	1.776(2)	1.763(3)	1.745(2)	—
Be–Y	1.6186(19)	1.6197(19)	1.626(2)	1.534(3)	1.557(2)	1.665(4)–1.667(4)
Y–C2	1.1674(17)	1.1740(17)	1.224(2)	1.273(5)	1.2626(19)	1.231(3)–1.234(3)
C2–E	1.6080(14)	1.6100(14)	1.5841(17)	1.531(5)	1.5575(16)	1.102(4)–1.138(4)
E–Be	—	—	—	—	—	1.693(4)–1.712(5)
max. (YCE)···Be$_{plane}$	*ca.* 0.28	*ca.* 0.40	—	*ca.* 0.38	*ca.* 0.41	
Be–Y–C2	170.42(12)	169.84(12)	144.73(13)	159.8(4)	132.99(13)	130.1(2)–131.6(2)
Y–C2–E	179.29(12)	178.73(13)	179.45(18)	177.5(6)	177.45(14)	177.3(3)–178.0(3)
C2–E–Be	—	—	—	—	—	167.1(3)–168.2(3)
Σ∠Be	359.99(11)	359.90(11)	—	359.94(16)	359.98(13)	—
|N1–C1–Be–Y|	110.1(1)	15.40(18)	—	113.43(19)	28.9(2)	16.9(4)–20.1(4)
|Z–C3–Be–Y|	63.8(2)	78.2(2)	51.3(2)	62.1(2)	114.3(2)	—
|N–C–Be–E|	—	—	—	—	—	96.7(3)–99.8(3)

^{a} YCE = NCS. ^{b} Z = N3. ^{c} Z = C4. ^{d} YCE = OCP. ^{e} Data for the only molecule of **3** in the asymmetric unit (out of 3), which does not display a disorder in the BeOCP moiety. ^{f} **4a** cocrystallised with 4% of leftover starting material **1a**, both molecules overlapping fully in the asymmetric unit, except for their Br/OCP ligands, which were freely refined, leading to relatively high esds. ^{g} YCE = OCN. ^{h} Structural data ranges provided for all three (CAAC)BBr(OCN) units present in the asymmetric unit. ^{i} n.d. = not determined.
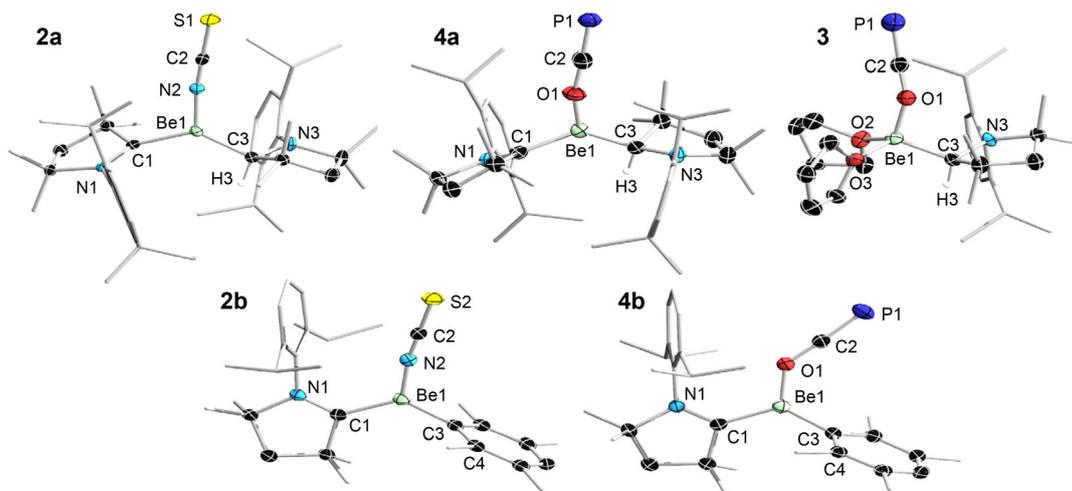
Fig. 2 Crystallographically determined solid-state structures of **1a**, **1b**, **3**, **4a** and **4b**. Atomic displacement ellipsoids at 50% probability. Minor disordered parts, lattice solvent molecules, ellipsoids of ligand periphery, and hydrogen atoms omitted for clarity, except for CAAC*H* protons.

minimise steric repulsion. The duryl substituent in **2b** is near-orthogonal to the beryllium plane (|C4–C3–Be1–N2| 78.2(2)°), but less so in **4b** (|C4–C3–Be1–O1| 62.1(2)°), perhaps to minimise repulsion between the π systems of the duryl ring and the C≡P moiety. The NCS and OCP moieties in **2a/b** and **4a/b**, respectively, approach linearity (N–C–S/O–C–P 177.45(14)–179.45(18)°) and are quasi-coplanar with the beryllium plane (S1/P1···Be$_{plane}$ < 0.41 Å).

The steric constraints imposed by the anionic CAAC*H*/Dur substituents have a significant impact on the orientation of the pseudohalide substituent relative to the CAAC ligand. In the duryl derivatives the NCS/OCP ligand tends towards coplanarity with the trigonal-planar CAAC carbene centre (**2b** |N1–C1–Be1–N2| 15.40(18); **4b** |N1–C1–Be1–O1| 28.9(2)°) in order to maximise overlap between the pseudohalide and CAAC π systems. In the CAAC*H* derivatives, however, the NCS/OCP ligand tends more towards orthogonality with the C1 plane as the much higher steric constraints override electronic effects (**2a** |N1–C1–Be1–N2| 110.1(1); **4a** |N1–C1–Be1–O1| 113.43(19)°).

Complexes **2a/b** are the first solid-state structures of tricoordinate beryllium thiocyanates. Accordingly, their Be1–N1 bonds (1.3011(15), 1.2967(16) Å) are necessarily shorter than those in the known tetracoordinate complexes (*ca.* 1.65–1.69 Å).[35,37] The Be–N2–C2 angle in **2a/b** deviates only slightly from linearity (*ca.* 170°), the NCS residue bending away from the CAAC and towards the CAAC*H*/Dur ligand. The N2–C2 (1.1674(17), 1.1740(17) Å) and C2–S1 (1.6080(14), 1.6100 (14) Å) bond lengths are typical for terminal beryllium thiocyanates (N–C *ca.* 1.14–1.17; C–S *ca.* 1.59–1.62 Å).[35,37]

Complexes **3**, **4a** and **4b** are the first examples of beryllium phosphaethynolates. The Be1–O1 bond lengths range from 1.534(3) to 1.626(2) Å, being longer in the tetrahedral complex **3** than in the trigonal-planar complexes **4a/b**. Furthermore, as Be1–O1 lengthens, O1–C2 shortens from 1.273(5) to 1.224(2) Å, while C2–P1 lengthens from 1.531(5) to 1.5841(17) Å, indicating small fluctuation in the degree of O=C=P character in

the predominantly O–C≡P resonance form. In the only four structurally characterised terminal s-block phosphaethynolates the O–C bonds (1.196(3)–1.207(4) Å) are significantly shorter, while the C–P bonds (1.555(4)–1.582(3) Å) fall within the same range as those in **3** and **4a/b**.[37,54,55] Whereas in **4a/b** the OCP substituent bends away from the CAAC ligand, the asymmetric unit of **3** contains two distinct topoisomers, one in which the OCP ligand points away from the CAAC ligand, the other towards. This is in agreement with the NMR data, which shows the presence of two rotamers, **3** and **3′**, in solution. The Be–O1–C2 angle in **3** and **4a/b** is much larger and varies more (132.99(13)–159.8(4)°) than the corresponding Be–N2–C2 angle in **2a/b**. In the literature-known s-block phosphaethynolates the M–O–C angle varies even more, from highly bent in [Na(OCP)(dibenzo-18-crown-6)] (138.1(2)°)[37] to nearly linear in [Na(OCP)(dme)$_2$] (107.7(3)°, dme = dimethyoxyethane),[55] but without apparent correlation with the O–C and C–P bond lengths and thereby the degree of O–C≡P character.

The centrosymmetric hexameric complex **7** crystallises in the chiral monoclinic space group *I*2/*a* (Fig. 3). The OCN ligands bridge between the six beryllium centres, forming a central 24-membered (BeOCN)$_6$ ring, within which the beryllium stereocentres alternate between the *R* and *S* configurations. Complex **7** is the first structurally characterised beryllium isocyanate and, to our knowledge, the largest known molecular (MOCN)$_n$ ring structure. The magnesium aluminate trimer [Me$_2$Al{μ-O(SiMe$_3$)}$_2$Mg(μ-OCN)]$_3$ presents a central 12-membered (MgOCN)$_3$ ring,[56]** while [(Cp^{iPr})U(μ-OCN)]$_4$ features a 16-membered (UOCN)$_4$ ring.[57] The Be–O (*ca.* 1.67 Å) and Be–N (*ca.* 1.70 Å) bond lengths are slightly longer than those in the tetrahedral phosphaethynolate **3** (1.626(2) Å) and known terminal beryllium thiocyanates (1.65–1.69 Å),[31–35]

The structural data for [Me$_2$Al{μ-O(SiMe$_3$)}$_2$Mg(μ-OCN)]$_3$ are of insufficient quality to allow comparison with **7.
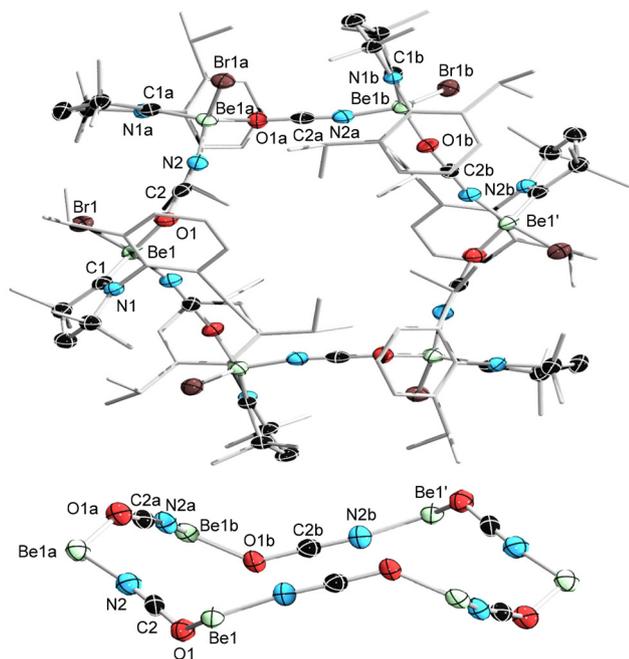
Fig. 3 Top: crystallographically determined solid-state structures of **7** (centrosymmetric hexamer). Atomic displacement ellipsoids at 50% probability. Ellipsoids of ligand periphery and hydrogen atoms omitted for clarity. Bottom: structure of the central $(BeOCN)_6$ ring of **7** (side view).

respectively. Each O–C–N–Be fragment is nearly linear (O–C–N *ca.* 178, C–N–Be *ca.* 168°), whereas the Be–O–C moieties are strongly bent (*ca.* 131°). The O–C (*ca.* 1.23 Å) and C–N (*ca.* 1.12 Å) bond lengths indicate a predominance of the O–C≡N resonance form. The only other structurally characterised s-block complex with an OCN unit bridging between two metal centres is an anionic magnesium porphyrin complex featuring an Mg–O–C–N–K linkage to the K^+ countercation, which shows significantly more pronounced O=C=N character (O–C 1.175(5), C–N 1.195(5) Å), resulting in much larger Mg–O–C (157.2(3)°) and much smaller C–N–K (123.1(3)°) angles.[58]

Finally, the tetrameric complex **8** also crystallises in the chiral monoclinic space group *I2/a* (Fig. S32 in the ESI†). The CN ligands bridge between the four beryllium centres, forming a central 16-membered $(BeCN)_4$ ring. This structural motif is relatively common, in particular in group 13 cyanide complexes,[59–62] but has never been reported for s-block complexes. Due to poor diffraction data quality and extensive structural disorders, structural parameters may not be discussed, but the data show that all four bridging cyano ligands are flip-disordered, as was already apparent from the solution NMR data (*vide supra*). This coordinative CN/NC isomerism is also observed in other structurally characterised cyanoberyllium complexes.[32,35]

Conclusions

The synthesis of well-defined beryllium-based pseudohalide Grignards from the CAAC-stabilised beryllium Grignards

[[(CAAC)(CAACH)BeBr] (**1a**) and [(CAAC)DurBeBr] (**1b**) has proven less straightforward than expected. With the exception of the first tricoordinate thiocyanate derivatives, [(CAAC)(CAACH)Be(η^1-NCS)] (**2a**) and [(CAAC)DurBe(η^1-NCS)] (**2b**), which are readily accessible by salt metathesis with [NaNCS], the syntheses of phosphaethynolate, isocyanate and cyanide derivatives are complicated by Schlenk-type ligand exchange and other undesirable side reactions. The syntheses of the OCP derivatives, in particular, are fraught with numerous side reactions, including scrambling of both the neutral and anionic ligands, OCP homocoupling, OCP coupling with the CAAC ligand, insertion of OCP into the Be–organyl bond, and ill-defined radical-generating redox processes. Nonetheless, the first examples of beryllium phosphaethynolates, tetracoordinate [(thf)₂(CAACH)Be(η^1-OCP)] (**3**) and tricoordinate [(CAAC)RBe(η^1-OCP)] (R = CAACH **4a**, Dur **4b**) were obtained and characterised by NMR and IR spectroscopy, as well as single-crystal X-ray crystallography. While attempts to obtain OCN derivatives also proved very unselective, fractional crystallisation yielded the first solid-state structure of a beryllium isocyanate, a hexameric complex featuring a unique $(BeOCN)_6$ ring, [(CAAC)BrBe(1,3-μ-OCN)]₆. Finally, attempts to synthesise a beryllium selenocyanate Grignard by salt metathesis with [Na/KSeCN] resulted instead in selenium abstraction by the CAAC ligand and the relatively selective generation of the tetrameric, self-stabilising mixed cyano/isocyanoberyllium Grignard [(thf)(CAACH)Be(1,3-μ-CN/NC)]₄. Overall, this study shows that CAAC ligands, which have enabled the isolation of numerous, otherwise inaccessible low-valent main group complexes,[46,63,64] are ill suited to the stabilisation of pseudohaloberyllium Grignards as they are easily displaced by THF, which is often required to solubilise the pseudohalide salt precursor, and may undergo side reactions with the pseudohalide substituents.

Data availability

Conflicts of interest

There are no conflicts to declare.

Acknowledgements

References

1   L. Birckenbach and K. Kellermann, *Ber. Dtsch. Chem. Ges. B*, 1925, **58**, 786.

2   F. Bellina and R. Rossi, *Chem. Rev.*, 2010, **110**, 1082.

3   M. R. Netherton and G. C. Fu, *Adv. Synth. Catal.*, 2004, **346**, 1525.

4   Y.-G. Chen, X.-T. Xu, K. Zhang, Y.-Q. Li, L.-P. Zhang, P. Fang and T.-S. Mei, *Synthesis*, 2018, **50**, 35.

5   S. Arlt, K. Bläsing, J. Harloff, K. C. Laatz, D. Michalik, S. Nier, A. Schulz, P. Stoer, A. Stoffers and A. Villinger, *ChemistryOpen*, 2021, **10**, 62.

6   P.-Y. Lin, A. Loganathan, I. Raifuku, M.-H. Li, Y.-Y. Chiu, S.-T. Chang, A. Fakharuddin, C.-F. Lin, T.-F. Guo, L. Schmidt-Mende and P. Chen, *Adv. Energy Mater.*, 2021, **11**, 2100818.

7   F. Cheng, J. Zhang and T. Pauporté, *ChemSusChem*, 2021, **14**, 3665.

8   C. Glidewell, *Inorg. Chim. Acta*, 1974, **11**, 257.

9   S. Harder and J. Langer, *Nat. Rev. Chem.*, 2023, **7**, 843.

10 A. Guérinot and J. Cossy, *Acc. Chem. Res.*, 2020, **53**, 1351.

11 Y. Nassar, F. Rodier, V. Ferey and J. Cossy, *ACS Catal.*, 2021, **11**, 5736.

12 C. E. I. Knappkea and A. Jacobi von Wangelin, *Chem. Soc. Rev.*, 2011, **40**, 4948.

13 S. R. Harutyunyan, T. den Hartog, K. Geurts, A. J. Minnaard and B. L. Feringa, *Chem. Rev.*, 2008, **108**, 2824.

14 J. L. Burmeister, *Coord. Chem. Rev.*, 1990, **105**, 77.

15 A. Tuulmets, M. Mikk and D. Panov, *Main Group Met. Chem.*, 1997, **10**, 1.

16 M. Hvastijová, J. Kohout, J. W. Buchler, R. Boča, J. Kožíšek and L. Jäger, *Coord. Chem. Rev.*, 1998, **175**, 17.

17 A. Klopsch and K. Dehnicke, *Chem. Ber.*, 1975, **108**, 420.

18 H. Böhland, F. R. Hofmann, W. Hanay and H. J. Berner, *Z. Anorg. Allg. Chem.*, 1989, **577**, 53.

19 A. D. Obi, H. R. Machost, D. A. Dickie and R. J. Gilliard, Jr., *Inorg. Chem.*, 2021, **60**, 12481.

20 D. Parveen, R. K. Yadav and D. K. Roy, *Chem. Commun.*, 2024, **60**, 1663.

21 M. R. Buchner, *Chem. – Eur. J.*, 2019, **25**, 12018.

22 K. J. Iversen, S. A. Couchman, D. J. D. Wilson and J. L. Dutton, *Coord. Chem. Rev.*, 2015, **297–298**, 40.

23 M. Arrowsmith, H. Braunschweig, M. A. Celik, T. Dellermann, R. D. Dewhurst, W. C. Ewing, K. Hammond, T. Kramer, I. Krummenacher, J. Mies, K. Radacki and J. K. Schuster, *Nat. Chem.*, 2016, **8**, 890.

24 J. T. Boronski, A. E. Crumpton, L. L. Wales and S. Aldridge, *Science*, 2023, **380**, 1147.

25 J. T. Boronski, A. E. Crumpton, A. F. Roper and S. Aldridge, *Nat. Chem.*, 2024, **16**, 1295.

26 C. Czernetzki, M. Arrowsmith, F. Fantuzzi, A. Gärtner, T. Tröster, I. Krummenacher, F. Schorr and H. Braunschweig, *Angew. Chem., Int. Ed.*, 2021, **60**, 20776.

27 G. Wang, J. Walley, D. Dickie, A. Molino, D. Wilson and R. J. Gilliard, *J. Am. Chem. Soc.*, 2020, **142**, 4560.

28 M. R. Buchner, L. R. Thomas-Hargreaves, C. Berthold, D. F. Bekiş and S. I. Ivlev, *Chem. – Eur. J.*, 2023, **29**, e202302495.

29 C. Helling and C. Jones, *Chem. – Eur. J.*, 2023, **29**, e202302222.

30 C. Czernetzki, T. Kunz, S. Huynh, A. Lamprecht, J. Sprenger, M. Finze, M. Arrowsmith and H. Braunschweig, *Angew. Chem., Int. Ed.*, 2024, **63**, e202401279.

31 H. Böhland, W. Hanay, M. Noltemeyer, A. Meller and H. G. Schmidt, *Fresenius' J. Anal. Chem.*, 1998, **361**, 725.

32 A. V. G. Chizmeshya, C. J. Ritter, T. L. Groy, J. B. Tice and J. Kouvetakis, *Chem. Mater.*, 2007, **19**, 5890.

33 B. Neumüller and K. Dehnicke, *Z. Anorg. Allg. Chem.*, 2007, **633**, 2262.

34 D. Naglav, D. Bläser, C. Wölper and S. Schulz, *Inorg. Chem.*, 2014, **53**, 1241.

35 C. Berthold, M. Müller, S. I. Ivlev, D. M. Andrada and M. R. Buchner, *Dalton Trans.*, 2023, **52**, 13547.

36 C. Czernetzki, M. Arrowsmith, L. Endres, I. Krummenacher and H. Braunschweig, *Inorg. Chem.*, 2024, **63**, 2670.

37 B. Neumüller and K. Dehnicke, *Z. Anorg. Allg. Chem.*, 2010, **636**, 1206.

38 R. J. Gilliard, Jr., D. Heift, J. M. Keiser, Z. Benko, A. L. Rheingold, H. Grützmacher and J. D. Protasiewicz, *Dalton Trans.*, 2018, **47**, 666.

39 Z. Li, X. Chen, M. Bergeler, M. Reiher, C.-Y. Su and H. Grützmacher, *Dalton Trans.*, 2015, **44**, 6431.

40 D. Heift, Z. Benko and H. Grützmacher, *Dalton Trans.*, 2014, **43**, 5920.

41 L. N. Grant, B. Pinter, B. C. Manor, H. Grützmacher and D. J. Mindiola, *Angew. Chem., Int. Ed.*, 2018, **57**, 1049.

42 D. W. N. Wilson, A. Hinz and J. M. Goicoechea, *Angew. Chem., Int. Ed.*, 2018, **57**, 2188.

43 J. M. Goicoechea and H. Grützmacher, *Angew. Chem., Int. Ed.*, 2018, **57**, 16968.

44 A. R. Jupp and J. M. Goicoechea, *Angew. Chem., Int. Ed.*, 2013, **52**, 10064.

45 J. K. Buchanan and P. G. Plieger, *Z. Naturforsch., B: J. Chem. Sci.*, 2020, **75**, 459.

46 S. Kundu, S. Sinhababu, V. Chandrasekhar and H. W. Roesky, *Chem. Sci.*, 2019, **10**, 4727.

47 G. Becker, G. Heckmann, K. Hubler and W. Schwarz, *Z. Anorg. Allg. Chem.*, 1995, **621**, 34.

48 W. Yang, K. E. Krantz, D. A. Dickie, A. Molino, D. J. D. Wilson and R. J. Gilliard, Jr., *Angew. Chem., Int. Ed.*, 2020, **59**, 3971.

49 B. Li, C. Wölper, H. M. Weinert, H. Siera, G. Haberhauer and S. Schulz, *Eur. J. Inorg. Chem.*, 2024, **27**, e202300622.

50 S. J. Urwin and J. M. Goicoechea, *Chem. – Eur. J.*, 2023, **29**, e202203081.

51 Y. Xiong, S. Yao, T. Szilvási, E. Ballestero-Martínez, H. Grützmacher and M. Driess, *Angew. Chem., Int. Ed.*, 2017, **56**, 4333.

52 D. W. N. Wilson, W. K. Myers and J. M. Goicoechea, *Dalton Trans.*, 2020, **49**, 15249.

53 M. Tretiakov, Y. G. Shermolovich, A. P. Singh, A. P. Samuel, H. W. Roesky, B. Niepötter, A. Visschera and D. Stalke, *Dalton Trans.*, 2013, **42**, 12940.

54 M. Westerhausen, S. Schneiderbauer, H. Piotrowski, M. Suter and H. Nöth, *J. Organomet. Chem.*, 2002, **189**, 643.

55 G. Becker, W. Schwarz, N. Seidler and M. Westerhausen, *Z. Anorg. Allg. Chem.*, 1992, **612**, 72.

56 H. Phull, D. Alberti, I. Korobkov, S. Gambarotta and P. H. M. Budzelaar, *Angew. Chem., Int. Ed.*, 2006, **45**, 5331.

57 M. A. Boreen, K. N. McCabe, T. D. Lohrey, F. A. Watt, L. Maron, S. Hohloch and J. Arnold, *Inorg. Chem.*, 2020, **59**, 8580.

58 K. Ezzayani, A. Ben Khelifa, E. Saint-Aman, F. Loiseau and H. Nasri, *Polyhedron*, 2016, **117**, 817.

59 M. Arrowsmith, D. Auerhammer, R. Bertermann, H. Braunschweig, G. Bringmann, M. A. Celik, R. D. Dewhurst, M. Finze, M. Grüne, M. Hailmann, T. Hertle and I. Krummenacher, *Angew. Chem., Int. Ed.*, 2016, **55**, 14464.

60 M. Molon, K. Dilchert, C. Gemel, R. W. Seidel, J. Schaumann and R. A. Fischer, *Inorg. Chem.*, 2013, **52**, 14275.

61 W. Uhl, T. Abel, E. Hagemeier, A. Hepp, M. Layh, B. Rezaeirad and H. Luftmann, *Inorg. Chem.*, 2011, **50**, 325.

62 W. Uhl and M. Matar, *Z. Naturforsch., B: J. Chem. Sci.*, 2004, **59**, 1214.

63 S. K. Kushvaha, A. Mishra, H. W. Roesky and K. Chandra Mondal, *Chem. – Asian J.*, 2022, **17**, e202101301.

64 M. Melaimi, R. Jazzar, M. Soleilhavoup and G. Bertrand, *Angew. Chem., Int. Ed.*, 2017, **56**, 10046.

65 D. Naglav, M. R. Buchner, G. Bendt, F. Kraus and S. Schulz, *Angew. Chem., Int. Ed.*, 2016, **55**, 10562.

66 M. R. Buchner and M. Müller, *ACS Chem. Health Saf.*, 2023, **30**, 36.